Mechanism for photoinduced structural phase transitions in low-dimensional electron-lattice systems: Nonlinearity with respect to excitation density and aggregation of excited domains

Kaoru Iwano
Institute of Materials Structure Science, High Energy Accelerator Research Organization, Graduate University for Advanced Studies, Oho 1-1, Tsukuba 305-0801, Japan
(Received 24 March 1999; revised manuscript received 23 July 1999)

We construct a model for photoinduced structural phase transitions, based on electron-lattice systems made of tunable number of chains. The ground state is chosen to be a charge-density wave at half filling. There the degeneracy of the ground states is lifted up in order to prepare two unequal states, namely, a stable one and a metastable one. The first important point is the nonlinearity, which means that more than one absorbed photon cooperatively drives the system into a semimacroscopic phase. In our model, we particularly assume that the system stays at a metastable state at the initial time. One absorbed photon tuned to the optical gap energy excites the electronic system to a charge-transfer state. After this photoexcitation, the system gradually relaxes to a self-trapped excitation state, but it still remains metastable because the conversion of the phase, namely, the reconstruction of charge distribution, is only local. With more than one absorbed photon, on the other hand, the channels to a global phase change open, and then the system changes into a stable ground state. Next, we study the condition that spatially separate excitations created by the photons aggregate with attractive forces. It is demonstrated by adiabatic potential-surface analyses and dynamical calculations that both the conditions, namely, those for the nonlinearity and the aggregation, are satisfied simultaneously in our model.

I. INTRODUCTION

In recent years the phenomena of photoinduced phase transitions have been attracting more and more attention.[1–5] In fact, the number of the materials in which the phenomena are confirmed is increasing year by year. Not only is the number increasing, but also we see a great variety in those materials. They range over various type of systems which are usually discussed in different contexts, such as conjugate polymers, charge-transfer salts, oxides, molecular crystals, and so on. Thus, these plenty of examples encourage the experimentalists to think that the phenomena will be ''general'' in the sense that they are not rare and can be observed if the materials are cleverly selected. It is also so for the theorists. Thus we start to develop a general theory of its mechanism in addition to studies of each specific material.

As a typical example of the phenomena, let us discuss one of the most prominent results, namely, that in a polydiacetylene (PDA).[1] This is a kind of conjugate polymer, made of alternating double and triple bonds of carbon in the main chain. This main chain itself is regarded as a one-dimensional (1D) insulator in which the absorption spectrum is interpreted using the concept of 1D excitons, whereas the structure of the side chains are rather complicated. In fact, there are many variations in the side chains, yielding many kinds of PDA's. What is important is the fact that they extend on both the sides of the main chain over rather long distances. Namely, this is not a simple 1D system at least from a viewpoint of the lattice structure. Moreover, these side chains play essential roles in the photoinduced phase transition. It is already accepted that the structural changes in the side chains along with those in the main one are the origin of the macroscopic phase conversion after laser irradiation, although the details are not clarified yet.

The next important feature of the photoinduced phase transition in the PDA is the nonlinearity. The curve of the photoconverted fraction as a function of the light intensity is not linear, but shows a sublinear tendency. This directly means that the absorbed photons are cooperatively working to induce the phase conversion. Similar nonlinearity is also confirmed in tetrathiafulvalene-*p*-chloranil (TTF-CA), a neutral-ionic-transition material.[2,3] There a threshold behavior is observed instead of a sublinear one, but we think that it is not necessary to distinguish them conceptually at present, because the latter might arise from some imperfections.

There is one more feature worth mentioning for the PDA. In this material, the photoinduced phase transition is reversible, that is, the initial metastable state (the low-temperature phase) is photoconverted to the stable state (the high-temperature phase), and then the latter is returned to the former again by photons. The latter part of the transition therefore proves that the transition is not due to heat accumulation. Another example is found in one of the manganese oxides. In $Pr_{1-x}Ca_xMnO_3$, the macroscopic structural change occurs by x ray.[4] It is free from a heat problem because the temperature there is well below the thermal transition temperature.

There were several theoretical studies in the past.[6,7] Almost all of them were based on a model of an assemblage of two-level systems. The nonlinearity was also investigated within the framework. Very recent studies have also used a similar model and performed dynamical calculations.[8] Although this type of model will be useful in treating almost isolated molecular systems, the electron itineracy is indispensable to study various systems as mentioned above. In particular, it is essential in describing electronic structures of excited states in a realistic manner. In this viewpoint, a two-dimensional charge-density-wave (CDW) model was investigated by Nasu.[9] However, that study treated only a rather

localized case with small itineracy. Moreover, the theoretical important points that will be mentioned later were not discussed in detail.

Keeping the above experimental cases in mind, in this article we develop a model for the photoinduced phase transition, as is mentioned at the beginning. We are here particularly interested in the transitions accompanying a structural change, because they are expected to survive for a long time of the order of μs. We therefore use an electron-lattice (el-l) model with finite electron itineracy. The Coulombic interaction between electrons will be rather relevant to the phase changes in a very short time scale. Even in a long time scale, it will affect the el-l motions and give variety to the dynamics, but it is beyond our scope here. Even within an el-l model, there are different situations. We here treat the half-filling case, because it is the simplest one. For example, in a model with a site-diagonal el-l coupling term, the ground state is a CDW. It is twofold degenerate if all the sites are originally equivalent. In this study, we add a special term to lift up the degeneracy. Then we have the two unequal states, namely, the true ground state and the metastable one. In the case of CDW, this special term corresponds to an energy difference between even- and odd-numbered sites. Here this is assumed to have a rather small value compared with the electron transfer energy. This should be interpreted as follows. The experimentally found photoinduced phase transitions occur within a rather small hysteresis loop at the thermal transition temperature,[1] which means that two phases with nearly equal free energies are competing with each other. We simulate such cases at zero temperature, using an energy difference of the order of several ten K, instead of tackling finite-temperature dynamics directly.

In a situation prepared in this way, we investigate photorelaxations from the metastable state to the stable one. We here focus on the low-dimensional systems because there are typical examples such as the PDA and TTF-CA. In particular, we are interested in 1D and 2D systems. Moreover, we prepare several cases as 1D systems: a tube or cylinder system with a finite diameter. In practice, they are realized by coupled chains with a periodic boundary condition (BC) in the chain-perpendicular direction. Increasing the diameter gradually from zero (1D) to infinity (2D), we can investigate the effect of geometry and dimension on the aforementioned nonlinearity, because the latter is deeply related to the shape and the formation energy of a domain wall separating two different phases. Thus our model makes it possible to simulate the dynamics of global phase changes at various ''strengths'' of the nonlinearity and learn a general tendency. The next theoretical point is the question how self-trapped excitations aggregate to one another. Here we use the word ''excitation'' instead of ''exciton,'' because there is no electron-hole (el-h) attraction in our model. With such excitations apart from each other, the above mechanism of nonlinearity does not work, because the accumulation of excited el-h pairs in a relatively small spatial region is assumed beforehand. Of course, there are cases in which the light intensity is high enough and excitations are condensed already at the beginning. However, even in that case, an attractive force between excitations is necessary to keep merged ones stable enough.

Based on the above points, we here describe our general expectations for single and coupled chains, and 2D systems. Being common to the chain systems, the formation energy of two domain walls is finite even with a short relative distance, and becomes constant when they are outside the mutual interaction. Then, in the ground state, the energy of a domain of a stable phase in a metastable background is equal to the energy gain due to the energy difference between the two phases, subtracted by that formation energy. When the size of the domain is small enough, the gain is negative by definition, or by the finite formation energy. While, in excited states, it is not so definite. Namely, it becomes a problem of energetics associated with the formation energy and the energy of each excitation, and so leads to the nonlinearity. For example, when the former is higher than the energy needed for the lowest one-photon excitation, the photon tuned to the optical gap energy never yields a global phase change. It is therefore very important that the formation energy of domain walls depends on its perpendicular size. We easily expect that the formation energy is proportional to the circumference of the cylinderlike system, i.e., the number of chains, which tendency gives stronger nonlinearity to coupled chains than to a single-chain system. In 2D systems, on the other hand, the formation energy is proportional to the linear size of a domain because domain wall is now a circle. It is expected that they have a larger potential barrier and hence much stronger nonlinearity.

As for the aggregations, it is important to expect what type of attractions will be working in each system. In the present study, we do not discuss those originating from Coulombic interactions through polarizations, because it is still hard to treat them in multiexcited states. In the presence of only el-l interactions, the mutual interactions between excitations are determined by geometrical conditions. In a single-chain system, two excitations nearby are bound with only one bond, and then it is impossible to make more than two excitations aggregate. Substantial aggregation is realized in coupled-chain systems with multibonds. These expectations are summarized and schematically illustrated in Fig. 1.

In this article, we are mostly concerned with a four-chain system, in which as many as four excitations are stably bound. Hence, the first part of our scenario is that two el-h pairs localized individually aggregate to form a unit with a higher energy. Next, such two units again form a larger unit with an attractive force. Namely, four excitations are assumed to aggregate. In the last part of the scenario, the nonlinearity finally works to cause a global structural change. This number of ''4'' is, of course, an example, but is motivated by the fact that the nonlinearity in the PDA is estimated to have an exponent near that number. Of course, there is another case in which the excitations occur stepwise. We do not deny such a possibility, but that might have less possibility than our scenario, because it is there assumed that the same electron is excited more than once.

The rest of this article is composed in the following way. In the next section, the model and the method for the calculation is briefly introduced. In the third and fourth sections, the above two points, i.e., the nonlinearity and the aggregation, are investigated by the analyses of the adiabatic potential surfaces, respectively. It is shown in the fifth section that these mechanisms really work in dynamical simulations. The last section is devoted to the conclusions and discussions.

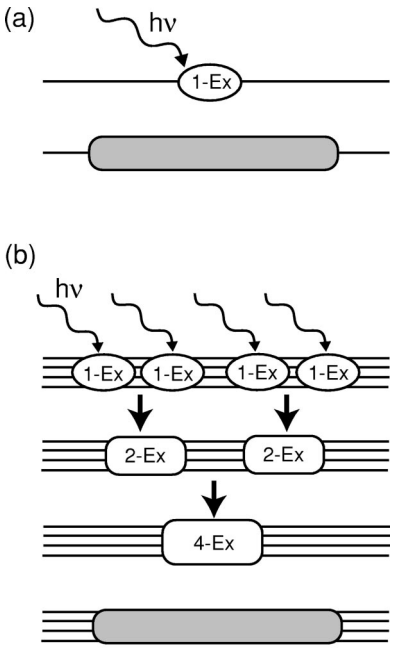

FIG. 1. A schematic illustration describing a typical case of photoinduced phase transition from a metastable phase to a stable one. (a): A single-chain case. Here ''1-Ex'' means an el-h pair which is locally self-trapped. Due to a relatively small formation energy of domain walls, even one photon can yield a stable phase as expressed by a shaded region. (b): A four-chain system. In a model later shown, four excitations (4-Ex) aggregate to form a seed for the transition.

II. MODEL AND METHOD

Throughout this article we utilize the following type of el-l model

$$H=-\sum_{(l,l')\sigma} t_0(C_{l\sigma}^{\dagger}C_{l'\sigma}+\text{H.c.})+\frac{\Delta}{2}\sum_l [1-(-1)^l]n_l + H_{e\text{-ph}}+\frac{m}{2}\sum_l \dot{Q}_l^2+\frac{K}{2}\sum_l Q_l^2, \tag{2.1}$$

where $C_{l\sigma}^{\dagger}$ and $C_{l\sigma}$ are creation and annihilation operators of an electron with σ spin at the lth site in a system of general dimension, and Q_l is the lth lattice displacement with mass m. The first term means the nearest-neighbor hopping with transfer energy t_0. The site energy Δ in the second term is introduced to lift up the degeneracy of the twofold ground states. In the cases with two directions, the factor $(-1)^l$ means $(-1)^{l_x}(-1)^{l_y}$, with $l=(l_x,l_y)$. Although we do not have a special real system in mind, it is necessary to fix the type of el-l coupling for practical calculations. In most of the calculations, we assume a site-diagonal term as

$$H_{e\text{-ph}}=-\alpha\sum_l Q_l(n_l-1). \tag{2.2}$$

In the following calculations, we use an adiabatic approximation to treat the lattice. Namely, we first calculate a rough sketch of adiabatic potential surfaces. This is very easy because we neglect electron-electron interactions here. As the next step, we solve the evolutional equations numerically. These equations consist of electronic time-dependent Shrödinger equations and classical equations of motion for the lattice, which are, in the case of the coupling (2.2),

$$i\hbar\frac{d}{dt}\psi_{\mu\sigma}(l)=(h)_{ll'}\psi_{\mu\sigma}(l') \tag{2.3}$$

with

$$(h)_{ll'}=\begin{cases}\dfrac{\Delta}{2}[1-(-1)^l]-\alpha Q_l & (l=l'),\\ -t_0 & (\text{nearest-neighbor } l \text{ and } l'),\end{cases} \tag{2.4}$$

and

$$m\frac{d^2}{dt^2}Q_l=-KQ_l+\alpha[\langle\Psi(t)|n_l|\Psi(t)\rangle-1], \tag{2.5}$$

respectively. Here $\psi_{\mu\sigma}(l)$ is the μth occupied wave function of an electron with spin σ, and $|\Psi(t)\rangle$ is the Slater determinant. In the cases of one or several chains, we use the open BC along the chain direction, but the periodic BC along the direction perpendicular to the chain. In a 2D case, on the other hand, the periodic BC is applied for both the directions. Next, we change the lattice variables to dimensionless ones as

$$q_l=\left(\frac{K}{\alpha}\right)Q_l, \tag{2.6}$$

and define the el-l interaction energy as

$$S=\frac{\alpha^2}{K}. \tag{2.7}$$

Then, scaling out the time variable by the lattice vibration frequency $\omega=\sqrt{K/m}$ as $u=t\omega$, the above evolutional equations are transformed into

$$i\frac{d}{du}\psi_{\mu\sigma}(l)=(\tilde{h})_{ll'}\psi_{\mu\sigma}(l'), \tag{2.8}$$

with

$$(\tilde{h})_{ll'}=\begin{cases}\left\{\dfrac{\Delta}{2}[1-(-1)^l]-Sq_l\right\}\Big/\hbar\omega & (l=l'),\\ -\dfrac{t_0}{\hbar\omega} & (\text{nearest-neighbor } l \text{ and } l'),\end{cases} \tag{2.9}$$

and

$$\frac{d^2}{du^2}q_l=-q_l+[\langle\Psi(u)|n_l|\Psi(u)\rangle-1]. \tag{2.10}$$

In real calculations, both the equations are solved step by step, using a time mesh as $\delta u=0.01$. In solving Eq. (2.8), the lattice variables are fixed at the values at that time, and then the evolution of the wave functions are easily calculated, using the basis set obtained by the diagonalization. The lattice Newtonian equation (2.10) is, on the other hand, solved by a midpoint method. We check the reliability by reversing the evolution or calculating the expectation value of the total energy defined as

$$E_{\rm tot}=\langle\Psi(u)|H_e(\{q_l\})|\Psi(u)\rangle+\frac{S}{2}\sum_l q_l^2+\frac{S}{2}\sum_l\left(\frac{dq_l}{du}\right)^2, \tag{2.11}$$

where

$$H_e(\{q_l\})\equiv-\sum_{(l,l')\sigma} t_0(C_{l\sigma}^{\dagger}C_{l'\sigma}+\text{H.c.}) + \frac{\Delta}{2}\sum_l [1-(-1)^l]n_l - S\sum_l q_l(n_l-1), \tag{2.12}$$

again in the case of the coupling (2.2). It should be emphasized here that our model has no term of energy dissipation. Thus, this total energy should be conserved. We avoid including the dissipation phenomenologically at this stage, because we want to know how the extra heat is released as a result of relaxation. However, the existence of dissipation is implicitly taken into account if it is necessary.

As the last remark of this section, we mention the strength of the el-l coupling parameter chosen in the following. When it is very large compared with t_0, the potential surfaces have many local minima, representing a localized nature of the system. For example, we find a different local minimum even when the distance between two domain walls is increased by one lattice constant. This leads to a situation where the relaxation ends at each attracting point, and hence many photons are needed for the formation of a sufficiently large domain. We therefore choose an *intermediate* coupling region all throughout this article.

III. NONLINEARITY

A. 1D system (a single-chain case)

First, as the simplest case, we discuss the feature of potential surfaces in a single-chain system. The chain length N is 100, being enough for the present purpose. The nondegeneracy parameter Δ is set to be 0.05 (hereafter all the energies are measured in the unit of t_0). We use the term in Eq. (2.2) with $S\equiv\alpha^2/K=1.1$. This choice of S gives a value near 0.75 as the CDW gap. Thus this belongs to an intermediate el-l coupling region. In Fig. 2(a), we show staggered lattice configurations, i.e., $(-1)^l q_l$. The lowest horizontal line drawn around $(-1)^l q_l=-0.4$ with structures on both the ends corresponds to the metastable state, while the stable one exists around the dashed line at $(-1)^l q_l=0.4$. Connecting these two states, we assume a one-parameter trajectory drawn in Fig. 2(a), which is expressed as

$$q_l=(-1)^l q_0\left\{1-q_{\rm D}\left[\tanh\left(\frac{|l-l_c|-\frac{1}{2}l_0}{w}\right)-1\right]\right\}, \tag{3.1}$$

where l_0, the only one parameter, specifies the kink-antikink distance. The other quantities are fixed at suitable values. Namely, q_0 is the CDW amplitude for the metastable state, and the depth of the deformation $q_{\rm D}$ is adjusted for the configuration to lead to the stable one. The half width of a kink

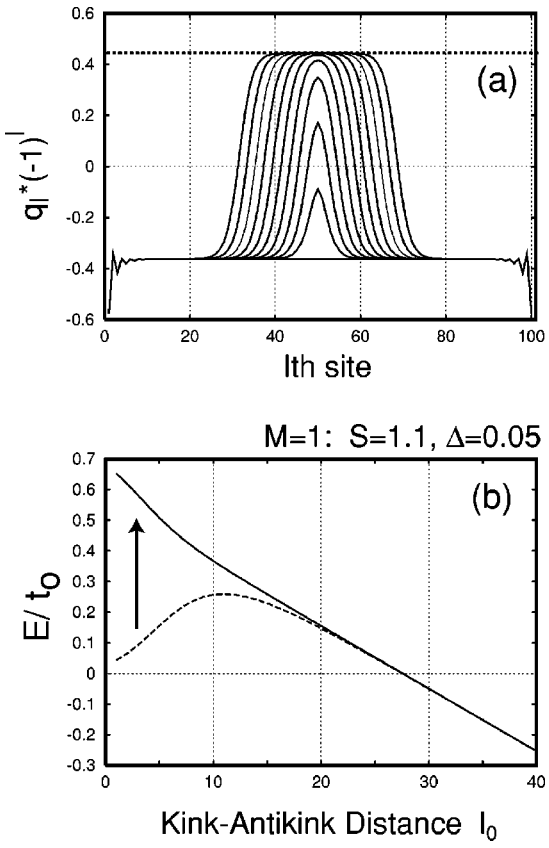

FIG. 2. (a) The staggered configurations of the lattice. The lowest horizontal line with structures on both the ends is that for the metastable state. The stable one is located around the dashed line near $(-1)^l q_l=0.4$. In between, kink-antikink type ones are assumed to connect both the extrema. (b) The adiabatic potential curves as functions of the kink-antikink distance l_0 in a single-chain system. The lower one is for the ground state, and the upper one for the first excited state. The energy is measured from the lowest energy in the metastable state (this definition is common to all the similar figures).

w is fixed at about 3.5, i.e., that of an isolated kink. The center of the kink-antikink pair is l_c, but the following result does not depend on its choice.

Using this trajectory, the potential curves for the ground state and the first excited one are shown in Fig. 2(b). Here and hereafter we measure the total energy from the lowest energy in the metastable state. By definition, the former one has a local minimum around $l_0=0$, i.e., the metastable state, with a potential barrier separating it from the stable state. In the first excited state, on the other hand, the surface has no barrier. This property in a single chain is easily understood by a similar tendency in a degenerate system.[10] Thus we can say that even one photon absorbed in the metastable state can drive the system into the stable state if there is no dissipation, which can be called *superlinear* nonlinearity.

B. 2D system

Next, we discuss a case in a 2D system. The system size is 20×20, which is again large enough to be considered as a 2D system in the following calculation. We use the same expression for the lattice trajectory, but with $l=(l_x,l_y)$. In

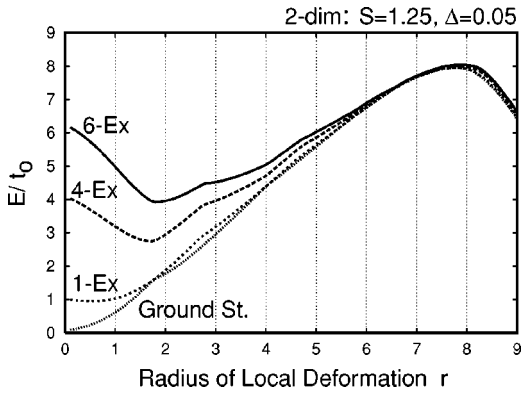

FIG. 3. The adiabatic potential curves as functions of the radius r of a local deformation in a 2D system. The abbreviation ''n-Ex'' means the *lowest* n-electron excitation state (this is used here and hereafter).

these configurations, the staggered lattice takes a deformation pattern similar to a pancake with a radius $r \equiv l_0/2$.

In Fig. 3, we show potential curves on various states. Here S and Δ are 1.25 and 0.05, respectively. The CDW gap is about 1.1. We use r as the only one parameter, with the other quantities fixed as in the previous way. For example, w is about 1.0. The abbreviations ''n-Ex'' on each curve means the *lowest* state of n-electron excitations. Of course, there are also other states, for example, higher one-electron excitations, and so on, but they are not shown. The reason is that we are interested in the phenomena where the lowest absorption edge is photoexcited. Generally speaking, higher-energy excitations will lead to easier phase conversion because of the increase in the relaxation channels. Although such cases are also interesting, they are not suitable for the present purpose of demonstrating the nonlinearity. It should be also mentioned that n-Ex $(n>1)$ states are embedded in the continuum of n'-Ex $(n'<n)$ states in some parts around $r=0$, although the latter are not explicitly shown in the figure. The mutual transitions among those states are properly considered in the dynamical calculations shown later. As for the potential surfaces themselves, there is a huge potential barrier between the metastable state and the stable one, even in the 1-Ex state. The origin of this barrier comes from the geometrical reason: the kink-antikink structure in 2D is nothing but a circular domain wall. Thus the total energy increases in a region where the radius is small, because the energy loss due to the formation of a domain wall is dominant. This barrier structure remains even in the 6-Ex state. Thus in this situation the phase conversion by photons is almost impossible. Of course, this property is directly related to the present selection of S and Δ, but it demonstrates how the dimensionality affects the nonlinearity when it is compared with the result in the previous 1D case.

C. 1D system (cases of more than one chain)

From the above results, we understand that the nonlinearity will be effectively controlled by the geometry of the system. Then we prepare systems which consist of more than one chain, namely, a cylinderlike system according to the present BC. The actual size is $N \times M$, with M as the circumference of the cylinder. We again use the expression in Eq. (3.1) with $l=(l_x,l_y)$, for the lattice trajectory. Since the center l_c is placed at the center of gravity of the cylinder, the pattern corresponds to two domain walls apart from each other with a distance l_0, each of which is localized around a cross section of the cylinder surface. The other quantities are again fixed in the same way as in the previous cases.

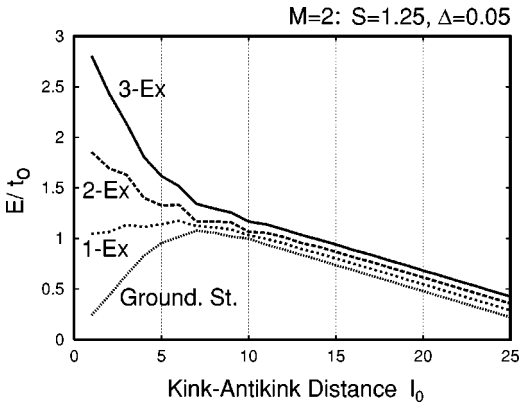

FIG. 4. Same as Fig. 2(b), but with $M=2$ (double chains).

In Fig. 4, we show the first example with $N=100$ and $M=2$. The values of S and Δ are 1.25 and 0.05, respectively. With this choice of S, the CDW gap is about 1.2. As seen from the figure, the overall structure of the potential curve has a slight barrier around $l_0=6$ for the 1-Ex state. While, it is barrierless for more than one-electron excitations. By the way, the curves are accompanied by small structures between sites. This comes from the so-called Peierls potential.

Increasing the number of M to four and changing the value of S to 1.1, we obtain another result in Fig. 5. Now the qualitative feature is very clear: the curve has a barrier up to the 3-Ex state, while no barrier for the 4- and 5-Ex states. To confirm the existence of the barrier, particularly, at the 3-Ex, we have tried an optimizing iteration (an overdamped dynamics) from a configuration around $l_0=0$, and found that the extension of the deformation stops just before the barrier point. Hence we expect that, when the dissipation, which is not included in our model, is strong enough, the structural change is limited to a local one in the former cases ($n=1$, 2, and 3). While, in the latter cases ($n \geq 4$), a global structural change can occur, whether the dissipation works or not. Thus we can say that this is a prototype to realize a *sublinear*

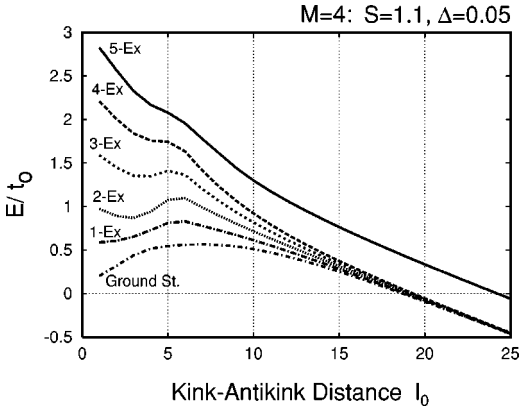

FIG. 5. Same as Fig. 2(b), but with $M=4$ (four chains).

nonlinearity. However, to conclude that this nonlinearity really works, there are still some questions. First, we must collect excitations in a rather small region, as already mentioned. This is discussed in the next section. Next, the dynamics in the 4-Ex state, for example, will be affected by remaining effects such as radiative and nonradiative transitions to smaller number of electron excitations. As for the former process, we must judge whether the time needed for the phase transition is short enough compared to a typical radiation life time of the order of ns. The latter one, on the other hand, is properly treated in the dynamical simulations.

IV. AGGREGATION

In this section, we investigate what kind of interactions are working between two local excitations, in order to clarify whether the aggregation really occurs.

A. Single-chain system

First, we study the system consisting of a single chain. The model and its parameters are the same as those corresponding in Sec. III, but we must focus on the excited states in the *stable* state. The reason is that the local excitations in the metastable state are all unstable for making local excitations. In fact, judging from Fig. 2, we expect a very fast formation of a kink-antikink pair even in the case of the lowest excitation.

Figure 6(a) shows the potential curve as a function of the distance between two localized 1-Ex's. Here the optimized lattice form of an isolated 1-Ex is assumed for each of them. The interaction is clearly attractive and its origin is similar to the binding force in a hydrogen molecule, as shown in Fig. 7(a). In this simple way of thinking, the lattice elastic energy is assumed to be almost constant or in the same tendency as the electronic energy. If we proceed with this way of thinking, it will be that the interaction is also attractive between a 2-Ex and a 1-Ex, and almost zero between two 2-Ex's, as shown in Figs. 7(b) and 7(c). However, the real potentials are only slightly attractive for the former, as shown in Figs. 6(b). Here we again assume a lattice pattern in which the optimized 1-Ex and 2-Ex are superimposed with a distance. A more detailed analysis shows that disappearance of appreciable attractive force comes from the increase in the electronic kinetic energy for a pair of excitations closer to each other. This is because an excited electron and a hole separated in each of the excitations should be confined in one region when a pair is merged. When we add one more 1-Ex to the slightly bound 3-Ex, the interaction then becomes attractive (dashed line), but it has a channel of dissociation, namely, the conversion into two 2-Ex's (solid line), as shown in Fig. 6(c).

Since our potential-curve analysis is based on somewhat restricted assumption for the configuration, we check the instability of a bound 4-Ex by the optimizing iteration. When we start the iteration from a distant pair of a 3-Ex and a 1-Ex, they come closer to each other, and then they actually dissociate into two 2-Ex's. In other words, the interaction between two 2-Ex's is *repulsive*, against the expectation at the beginning. Thus the aggregation of excitations never proceeds beyond two excitations in a single-chain system.

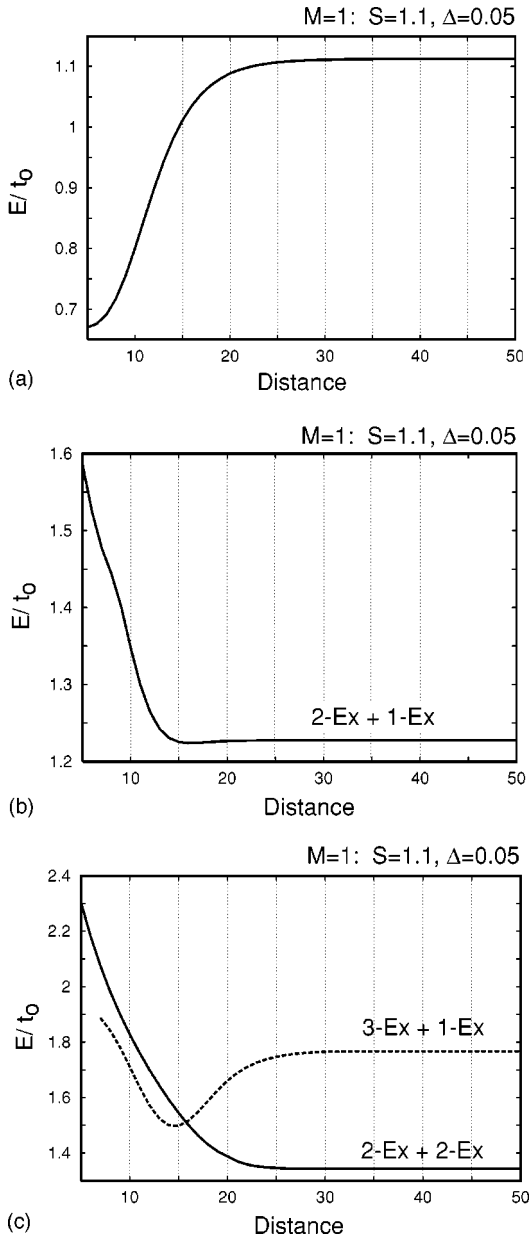

FIG. 6. (a) The 2-Ex potential curve as a function of the distance between a 1-Ex and another 1-Ex. (b) The 3-Ex potential curve as a function of the distance between a 2-Ex and a 1-Ex. (c) The 4-Ex potential curve as a function of the distance between a 1-Ex and a 3-Ex (dashed line), and the same curve as a function of the distance between a 2-Ex and another 2-Ex (solid line).

B. Four-chain system

Next, we investigate a system of four chains, from the same viewpoint. The model and the parameters are the same as those corresponding in Sec. III. In Fig. 8(a), we show the potential curve as a function of the distance between two localized 1-Ex's. The overall structure is attractive, although it is not so monotonic as that in a single-chain system. We return back to this point later.

The interaction between 2-Ex's is clearly *attractive*, as seen in Fig. 8(b). The origin of this attractive interaction is schematically explained in Fig. 7(d). Namely, we have more than one ''bond'' for binding, due to the coupled chains. This makes it possible that all the excited electrons and the

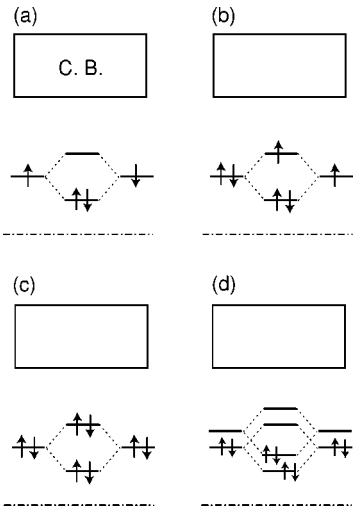

FIG. 7. Schematic electronic level structures. Considering the el-h symmetry, we only show the upper half part above the gap center. From (a) to (c), a single-chain system is assumed. The total number of excited electrons changes from 2 to 4, respectively. While, in (d), we illustrate the case where four electrons are excited in a four-chain ($M=4$) system. Notice that an attractive interaction is possible in the last case, because of the ''multibond mechanism.''

holes are contained in bonding orbitals. There is a little complicated structure for a small distance, but it is not important because we are now thinking about a situation where two 2-Ex's are initially apart from each other. It is also worth mentioning that the minimum point has a configuration similar to that of the 4-Ex at $l_0=6\sim7$, in Fig. 5. Thus it is conjectured that the phase convergence can occur after two 2-Ex's come closer to each other and get merged.

V. DYNAMICS

In this section we demonstrate how the predictions in the previous sections are realized in the dynamical calculations performed using the method in Sec. II. All through this section, we use a small value for the lattice frequency, i.e., $\omega=0.005$. One reason for this choice is of course to give an adiabatic situation consistent with the potential-surface analyses performed in the previous sections. In particular, our proposed mechanism needs no tunneling effect through barriers, and so the quantum effect can be neglected in that sense.

A. Single-chain system

First we treat the single-chain system in order to understand common and basic features of the dynamics, before discussing the main points. Again, the same model for a single chain as those in Secs. III and IV is used with the same parameters. Here we investigate a situation where the metastable state is photoexcited as expressed by the arrow in Fig. 2. As is already discussed, we expect that even the excitation to the lowest excited state makes it possible for the whole system to relax down to the stable state. Figure 9(a) shows some snapshots of the staggered lattice. The initial state, drawn by the dashed line, is assumed to be a small deformation. This assumption will need an explanation. Since the state just after the photoexcitation is a free el-h

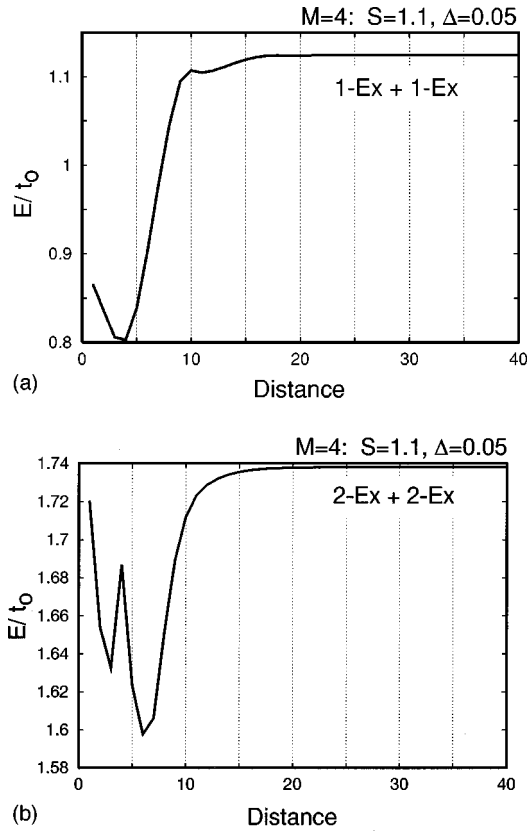

FIG. 8. (a) The 2-Ex potential curve as a function of the distance between a 1-Ex and another 1-Ex, in the case of a four-chain ($M=4$) system. (b) The 4-Ex potential curve as a function of the distance between a 2-Ex and another 2-Ex.

pair, there always should be a translational symmetry. This symmetry is important particularly when we discuss the very early stage of the relaxation from the free el-h state. It is, however, an unsolved problem to treat that stage correctly in 1D systems. Thus we here put aside that and start our simulation from this slightly localized state because our concern here is not to determine the transition probability correctly, but to understand the tendency of the dynamics.

Returning to the figure, it is easily seen that the system is being converted to the stable state. This conversion is driven by the moving kink and antikink. If we compare the snapshots at different times, we notice that the kinks have almost constant velocities. Since the conservation of the total energy holds with a very small deviation (less than 10^{-5}) in this simulation, this means that the released energy has flown to the other vibrational modes except for the center-of-gravity motion of each kink. In fact, it is stored in the particular vibrational mode, which appears as the oscillations in the converted part, as seen in the lattice pattern. To make it more transparent, we show a Fourier transform of a fraction of the wavy part. Here only the real part is plotted in Fig. 9(b). The central peak is nothing but the Peierls mode with the wave number of $k_0=2k_F$, and the second largest ones have $k=k_0\pm2\pi/\lambda$ with λ as nearly twelfth times the lattice constant. Since this λ is almost the same as the kink width (see the snapshots), we think that this mode is closely related to the kink itself, although the detail is not clear at this stage. Anyway, we can say that the released energy is not distributed evenly to almost all the vibrational modes, in other

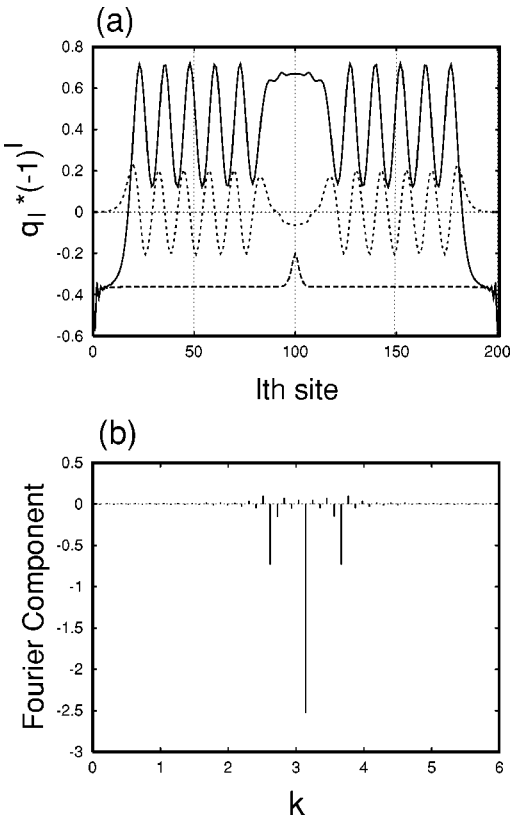

FIG. 9. (a) A snapshot of the lattice configuration (solid line) and its velocity (dotted line) at $t=60/\omega$. For both, the staggered field is shown. The initial configuration is specified by the dashed line, while the initial electronic state is a 1-Ex. (b) The real part of the Fourier component of the configuration (solid line), as a function of the wave number k. Only the region of $l=121-180$ is analyzed.

words, not as heat. Moreover, we have tried other initial conditions by changing the initial depth of the deformation to confirm that the result is always similar. Then, to know whether this is not an effect special to this model, but a general behavior, we also perform a similar simulation in a different type of el-l model, namely, a Su-Schrieffer-Heeger (SSH) model[11] with nondegenerate ground states:

$$H_{\mathrm{SSH}}=-\sum_{(l,l')\sigma}\left(t_0-\beta(Q_{l+1}-Q_l)+\frac{\Delta'}{2}[1-(-1)^l]\right)\times(C_{l\sigma}^{\dagger}C_{l'\sigma}+\mathrm{H.c.})+\frac{m}{2}\sum_l \dot{Q}_l^2+\frac{K}{2}\sum_l (Q_{l+1}-Q_l)^2, \tag{5.1}$$

where β means the site-*off*-diagonal el-l coupling, and Δ' is the nondegeneracy parameter. Again, changing the lattice variable to dimensionless one as $q_l=(K/\beta)Q_l$, the el-l coupling parameter is redefined so as to have the dimension of energy, as $S'=\beta^2/K$. As is well known, this model has degenerate ground states of a bond-order wave (BOW) for the half-filling case, if $\Delta'=0$. Taking values of Δ' and S' as 0.05 and 0.5, respectively, we obtain the result of the simulation in Fig. 10. Here we have plotted the bond variable y_l

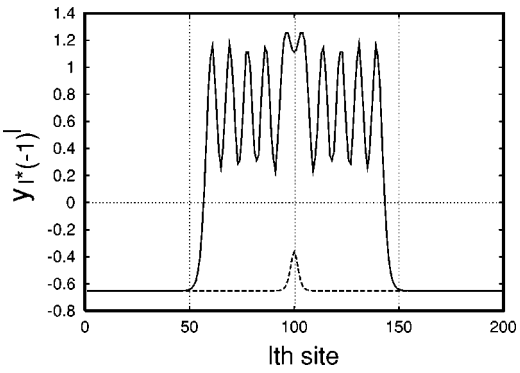

FIG. 10. A snapshot of the lattice configuration (solid line) at $t=20/\omega$, in the case of the SSH model. Again the initial configuration is depicted by the dashed line.

$\equiv q_{l+1}-q_l$, instead of q_l itself. Then we clearly see that a similar selection of a mode is occurring although the wave length of the selected mode is now shorter than the previous case, representing a shorter kink width. This special behavior seems to be related to a breather in the degenerate case[12] ($\Delta'=0$). A breather has a finite spatial size and a constant energy, while the present structure is growing with time. In this sense, the latter can be called a reminiscent of a breather.

Generally speaking, we think that this mode selection, or a nonergodicity, will be important at least in the following two senses. First, this will make the phase conversion easier, even if the original state, i.e., the metastable one, is the high-temperature phase, because the inverse conversion due to the increase in the temperature is suppressed. Next, the selection

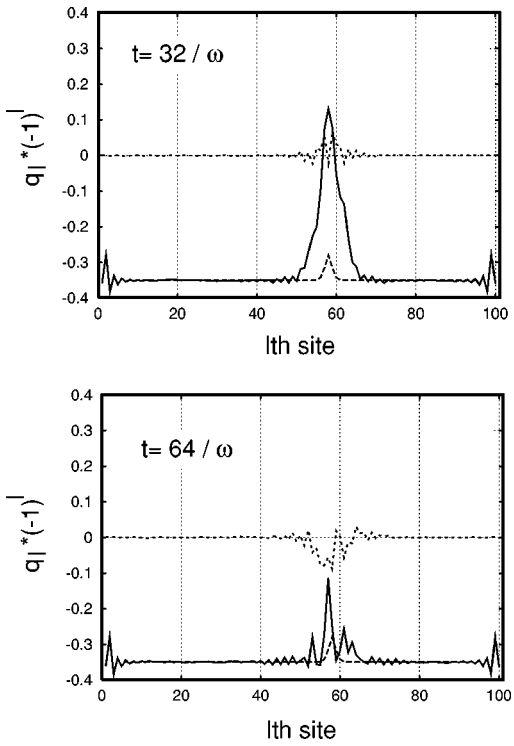

FIG. 11. Snapshots of the lattice configuration at $t=32/\omega$ and $64/\omega$, in the case of a four-chain ($M=4$) system. The meaning of each line follows those in Fig. 9, but only the configuration in a certain chain is shown for simplicity. The initial electronic state is a 1-Ex.

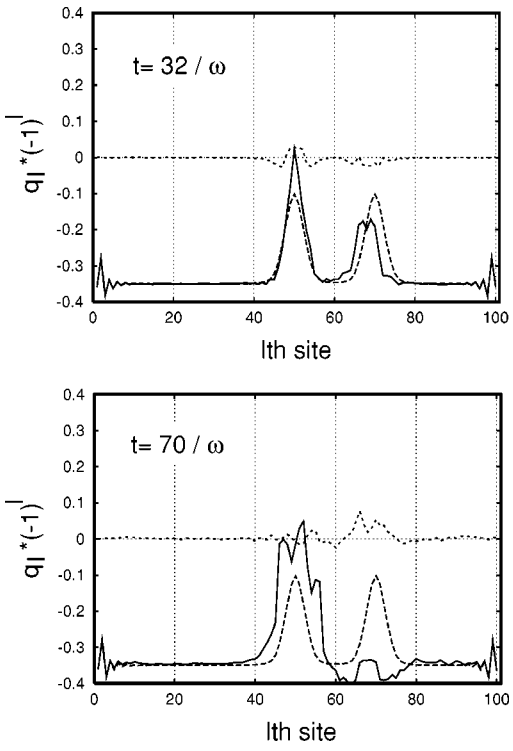

FIG. 12. Same as Fig. 11, but with a 2-Ex as the initial electronic state.

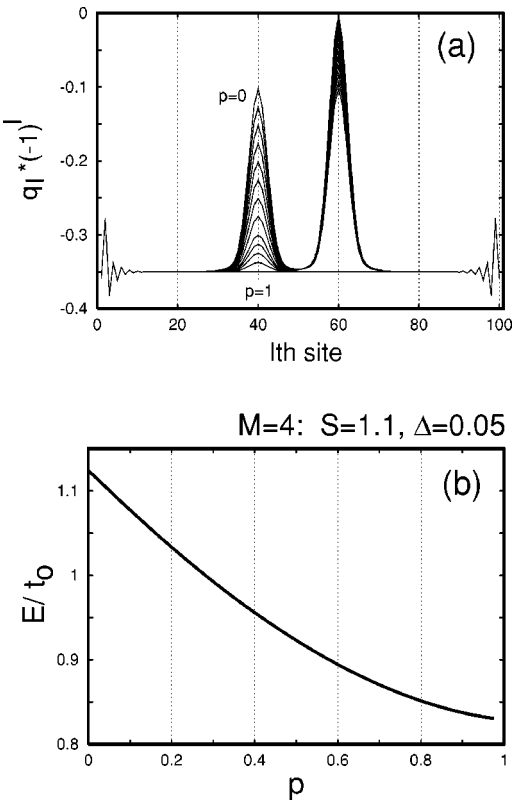

FIG. 13. Another relaxation channel for a pair of 1-Ex's. (a) An assumed one-parameter trajectory of the staggered lattice field. By definition, the two deformations are equivalent when the parameter p is zero. In increasing p, one of each grows, and, accordingly, the other becomes smaller and finally vanishes at $p=1$. (b) The total-energy curve as a function of p.

of the special vibrational mode seems to be related to the internal structure of the domain wall. This might give a possibility to study the nature of the domain walls through optical properties such as transient absorption spectra.[5]

B. Four-chain system

Next, we discuss the dynamics in a four-chain system, whose model and parameters are completely the same as those corresponding in Secs. III and IV. The first example is the case where the initial state is a small deformation on the 1-Ex. In Fig. 11, the snapshots at $t=32/\omega$ and $64/\omega$ are shown. There the staggered lattice field remains localized with an oscillatory behavior. Since the optical gap energy is smaller than the barrier height measured from the Franck-Condon ground state, it is very natural that there occurs no phase conversion. We have also checked the mixing effect between the electronic levels, but it is negligible.

We then proceed to the case in the 2-Ex. Here we choose the initial condition to be a pair of 1-Ex's, apart from each other as drawn by the dashed line in Fig. 12. Each of these 1-Ex's is assumed to be already relaxed individually. At $t=32/\omega$ (upper one), they are slightly approaching to each other, as expected from the potential surface. More importantly, they are no longer equivalent, in spite of the same initial shape. This tendency is more conspicuous after a longer time, for example, $t=70/\omega$ (lower one). There the left-hand excitation is almost similar to a locally relaxed 2-Ex (see Fig. 14), while the right-hand one seems to be almost vanishing although local oscillations are still remaining. This result suggests another channel of relaxation, namely, not a merging accompanying the lattice, but that triggered by a pure electronic transfer from one excitation to the one nearby. Thus we are tempted to draw one more potential curve in the 2-Ex, i.e., Fig. 13(b). Here the parameter p measures the trajectory changing from two neighboring 1-Ex's ($p=0$) to one 2-Ex ($p=1$), as shown in Fig. 13(a). As is clearly seen, the potential curve is monotonically decreasing from the former to the latter, which confirms our expectation. The ''equivalent'' merging, on the other hand, seems to occur with less possibility, because the potential curve is not so monotonic, as already pointed out in Fig. 8(a). Here the reader might have a question how the symmetry breaking related to the parity has occurred. In our simulation, which treats the lattice classically, it is incorporated by placing the center of gravity of the initial deformation between sites. This is not so artificial, because there will be many parity-breaking imperfections in real materials. Moreover, if we treat the lattice quantum-mechanically, such a relaxation becomes possible even in a regular system, due to the emission of odd-parity phonons. During such a process, the true state should be expressed by the linear combination of the two possible states: the one in which an electronic excitation is transferred from the left to the right, and vice versa. As for the phase conversion, it is not realized in this simulation, representing the existence of the energy barrier discussed in Sec. III.

As the last example, we investigate the most important case, a relaxation process in the 4-Ex. We start our simulation from a pair of 2-Ex's, which are apart from each other at the initial time, as shown in Fig. 14 (see the dashed line). Each of them is prepared to have the optimized shape of the

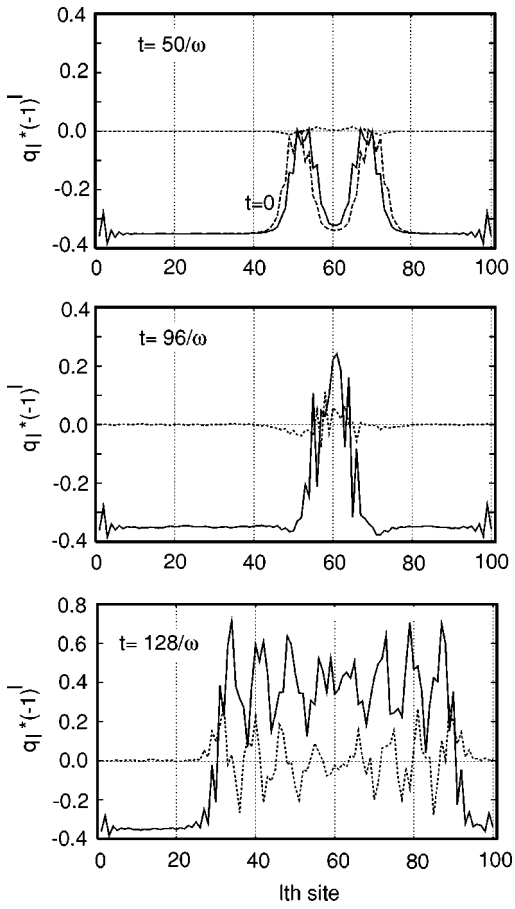

FIG. 14. Same as Fig. 11, but with a 4-Ex as the initial electronic state.

isolated one. Being different from that for the 1-Ex, it contains a long-wave component in addition to the staggered one. At $t=50/\omega$ (top), we see that they are approaching each other, judging from the staggered pattern and velocity. After a while, they get almost merged, as shown in the middle snapshot at $t=96/\omega$. Finally, in the bottom one at $t=128/\omega$, the expected phase conversion is really occurring. We again notice an oscillatory behavior in the converted part of the lattice. This has the same origin as those in Figs. 9(a) and 10, but is now rather complicated due to chain coupling. To know the degree of the level mixing, we have made a detailed analysis of the electronic wave functions at $t=96/\omega$, because it is not relevant at later times. The result is about 20%. Namely, among four excited electrons, nearly one electron has decayed to the lower levels. This decay itself, however, accelerates the phase conversion, at least, just after the decay, because the released energy is transformed to the lattice kinetic energy. We think that this is why the phase conversion has been realized in the present case, in spite of the one-electron decay.

Lastly, we mention another explanation for the different behaviors seen for the 2-Ex and 4-Ex. As shown in Fig. 7(d), the lower two levels on the left- and right-hand sides are all occupied by excited electrons in the case of the 4-Ex. Therefore there occurs no pure electronic transition between the left and the right. While, in the case of 2-Ex, there are only two excited electrons, i.e., one for each side, and so the transition between them is possible.

VI. CONCLUSIONS AND DISCUSSIONS

We have proposed a scenario for the photoinduced structural phase transitions. In that scenario, we start from a situation where individual excitations are already relaxed by themselves. As far as the concentration is low and they are apart from each other, it is almost the same as in conventional insulators, and so nothing special happens. However, with increased light intensity, two of them happen to be nearby. Then, they come closer to each other and get merged, due to an attractive force. Still, such a deformation is local. This comes from a rather strong nonlinearity which suppresses a global lattice change triggered by a small deformation. Therefore we assume again an attractive force between merged excitations, to form a larger unit of excitations. In our scenario, this plays the role of a seed for the photoinduced structural phase transition and makes the original phase unstable in a global region of the system.

To realize the above scenario, we need, at least, two necessary conditions: the nonlinearity and the aggregation of the excitations. From the analyses of adiabatic potential surfaces, we predict that both the conditions are satisfied simultaneously by an appropriate el-l model made of coupled chains. There the system is prepared to have nondegenerate CDW ground states, and then we assume that the lowest absorption edge above the CDW gap is photoexcited in the metastable state. To demonstrate that our model really works for the purpose, we have also performed dynamical calculations, in which the lattice is treated classically, while the electrons full-quantum mechanically. Choosing a low vibrational frequency which is consistent with the assumption of a classical lattice, we actually observe the aggregation of the excitations, and the phase conversion afterward. In that simulation, we have not included the effect of extrinsic dissipation. One of the reasons is that we are interested in the flow of released energy from kink motions to other vibrational modes. The result shows that selections of specials modes are common to both single- and coupled-chain systems. Moreover, the proposed mechanism does not include any tunneling or overpassing effect related to potential barriers. Therefore the existence of extrinsic dissipation does not matter here.

The time needed for the whole process of this conversion depends on the initial excitation densities determined by the light intensity. In this study, we have confined ourselves to estimate the time needed for the elementary processes, namely, the merging of excitations which are initially located nearby, and the formation of a seed for the phase conversion. In the case of the four-chain system, two 1-Ex's, which are initially placed with a mutual distance of about twice their size, have merged within $70/\omega$. Also, almost the same length of time is found to be enough for the merging of two 2-Ex's into a seed. Since $100/\omega$ is about 10 ps if $\hbar\omega$ is 0.005 eV, this is much shorter than typical radiation life times of the order of ns. Moreover, the radiation life time is expected to become longer and longer as the kink-antikink structure grows to have a larger kink-antikink distance, because the radiative decay to the ground state occurs as a result of the electron transitions between the two kinks.

In the rest of this section, we mention some future prob-

lems. In this article, we have only treated the cases where the metastable phase is photoexcited. However, another case, namely, the excitation in the stable phase, can also induce a phase conversion in real materials.[1–3] Although the conversion of such a case is not so drastic, it is also very important in the sense that a phase which is not realized thermally can be created by photons. Another remaining point is the derivation of the exponent of the nonlinearity. Our approach here still stays at the level of identifying elementary processes. The next step is then to perform a simulation in systems of a larger size, in order to evaluate statistical quantities.

ACKNOWLEDGMENTS

The author expresses his sincere gratitude for valuable experimental information from Professor S. Koshihara, Professor K. Tanimura, Professor K. Hashimoto, Professor H. Okamoto, and Dr. M. Fiebig. He is also thankful for fruitful discussions with Professor K. Nasu. This work was supported by the Grant-in-Aid (No. 10640319) for Scientific Research from the Ministry of Education, Science, Sports and Culture of Japan. Lastly, a part of the numerical calculations were performed using the Facom VPP500 at the computer center of KEK.

[1] S. Koshihara, Y. Tokura, K. Takeda, and T. Koda, Phys. Rev. Lett. **68**, 1148 (1992); Phys. Rev. B **52**, 6265 (1995).

[2] S. Koshihara, Y. Tokura, T. Mitani, G. Saito, and T. Koda, Phys. Rev. B **42**, 6853 (1990); S. Koshihara, Y. Takahashi, H. Sakai, Y. Tokura, and T. Luty, J. Phys. Chem. B **103**, 2592 (1999).

[3] K. Tanimura (unpublished).

[4] K. Kiryukhin, D. Casa, J.P. Hill, B. Keimer, A. Vigliante, Y. Tomioka, and Y. Tokura, Nature (London) **386**, 813 (1997).

[5] M. Fiebig (unpublished).

[6] E. Hanamura and N. Nagaosa, J. Phys. Soc. Jpn. **56**, 2080 (1987).

[7] N. Nagaosa and T. Ogawa, Phys. Rev. B **39**, 4472 (1989).

[8] K. Koshino and T. Ogawa, J. Phys. Soc. Jpn. **67**, 2174 (1998); Phys. Rev. B **58**, 14 804 (1998).

[9] K. Nasu, in *Relaxations of Excited States and Photo-Induced Structural Phase Transitions*, edited by K. Nasu (Springer-Verlag, Berlin, 1997), p. 3.

[10] S. Kivelson and W.-K. Wu, Phys. Rev. B **34**, 5423 (1986).

[11] W.P. Su, J.R. Schrieffer, and A.J. Heeger, Phys. Rev. Lett. **42**, 1698 (1979); Phys. Rev. B **22**, 2099 (1980).

[12] A.R. Bishop, D.K. Campbell, P.S. Lomdahl, B. Horovitz, and S.R. Phillpot, Phys. Rev. Lett. **52**, 671 (1984).